Developmental Cell
Article

Polycomb Group Proteins Ezh2 and Rnf2 Direct Genomic Contraction and Imprinted Repression in Early Mouse Embryos

Rémi Terranova,[1] Shihori Yokobayashi,[1] Michael B. Stadler,[1] Arie P. Otte,[2] Maarten van Lohuizen,[3] Stuart H. Orkin,[4] and Antoine H.F.M. Peters[1,*]
[1]Friedrich Miescher Institute for Biomedical Research, Maulbeerstrasse 66, CH-4058 Basel, Switzerland
[2]Swammerdam Institute for Life Sciences, University of Amsterdam, Kruislaan 406, 1098 SM Amsterdam, The Netherlands
[3]Division of Molecular Genetics and Centre for Biomedical Genetics, The Netherlands Cancer Institute, Plesmanlaan 121, 1066 CX Amsterdam The Netherlands
[4]Department of Pediatrics, Division of Hematology/Oncology, Children's Hospital, the Dana Farber Cancer Institute, Harvard Medical School, Boston, MA 02115, USA
*Correspondence: antoine.peters@fmi.ch
DOI 10.1016/j.devcel.2008.08.015

SUMMARY

Genomic imprinting regulates parental-specific expression of particular genes and is required for normal mammalian development. How imprinting is established during development is, however, largely unknown. To address this question, we studied the mouse *Kcnq1* imprinted cluster at which paternal-specific silencing depends on expression of the noncoding RNA *Kcnq1ot1*. We show that *Kcnq1ot1* is expressed from the zygote stage onward and rapidly associates with chromatin marked by Polycomb group (PcG) proteins and repressive histone modifications, forming a discrete repressive nuclear compartment devoid of RNA polymerase II, a configuration also observed at the *Igf2r* imprinted cluster. In this compartment, the paternal *Kcnq1* cluster exists in a three-dimensionally contracted state. In vivo the PcG proteins Ezh2 and Rnf2 are independently required for genomic contraction and imprinted silencing. We propose that the formation of a parental-specific higher-order chromatin organization renders imprint clusters competent for monoallelic silencing and assign a central role to PcG proteins in this process.

INTRODUCTION

In placental mammals, genomic imprinting ensures the strict parent-of-origin-specific expression of about 80 currently known imprinted genes. The majority of these genes are involved in placental and embryonic development or in postnatal neurological processes. Most imprinted genes are localized in multigene clusters in which monoallelic expression is controlled by a *cis*-acting imprinting control region (ICR). ICRs are marked by DNA methylation acquired during preceding oogenesis or spermatogenesis. At the *H19-Igf2* imprinted cluster, parental-specific DNA methylation at the ICR directs silencing in *cis* via a CTCF-mediated insulator mechanism (Kurukuti et al., 2006; Murrell et al., 2004). At the *Kcnq1* and *Igf2r* imprinted clusters, however, expression of the *Kcnq1ot1* and *Air* long noncoding RNAs (ncRNA) from the unmethylated paternal alleles is required for silencing in *cis* (Fitzpatrick et al., 2002; Mancini-Dinardo et al., 2006; Sleutels et al., 2002). Although widely discussed (Pauler et al., 2007; Umlauf et al., 2008), it is not known whether *Kcnq1ot1* and *Air* ncRNAs mediate repression in *cis* by forming a repressive nuclear compartment devoid of RNA polymerase II (RNAP), like *Xist* during X inactivation (X_i) (Chaumeil et al., 2006), or whether transcription through the ncRNA locus per se is required for imprinted silencing in *cis*.

Here, we study the *Kcnq1* imprinted gene cluster as a model system to unravel the molecular mechanisms by which ncRNAs and epigenetic modifiers cooperate to mediate monoallelic gene silencing during mammalian development. Recent studies point to differential regulation of genes along the 1 Mb *Kcnq1* genomic cluster (Lewis et al., 2004, 2006; Shin et al., 2008; Umlauf et al., 2004; reviewed in Peters and Schubeler, 2005). Whereas so-called "inner" genes are ubiquitously imprinted in embryonic and extraembryonic tissues, "outer" genes are imprinted exclusively in extraembryonic tissues in the absence of promoter DNA methylation (Figure 1A) (Lewis et al., 2004; Schulz et al., 2006). In extraembryonic tissues at 9.5 days of development, H3 lysine 27 trimethylation (H3K27me3), a mark mediated by the evolutionary conserved Polycomb repressor complex 2 (PRC2), is enriched throughout the paternal *Kcnq1* cluster (Umlauf et al., 2004), suggesting a role for PRC2-dependent mechanisms in regulating genomic imprinting. Consistently, paternal repression of *Cdkn1c* was partly alleviated in E7.5 embryos deficient for the PRC2 component *Eed* (Mager et al., 2003). PRC1 is thought to cooperate with PRC2 to mediate repression by inhibiting chromatin remodeling, blocking transcription through Rnf2-mediated H2A lysine 119 monoubiquitination (H2AK119u1), and by mediating chromatin compaction (Levine et al., 2004; Stock et al., 2007; van der Stoop et al., 2008). Whether PRC1 is involved in regulating imprinted silencing is still unknown. The repressive H3K9me2 and H3K9me3 modifications are also enriched at paternally imprinted genes within the *Kcnq1* cluster (Umlauf et al., 2004).

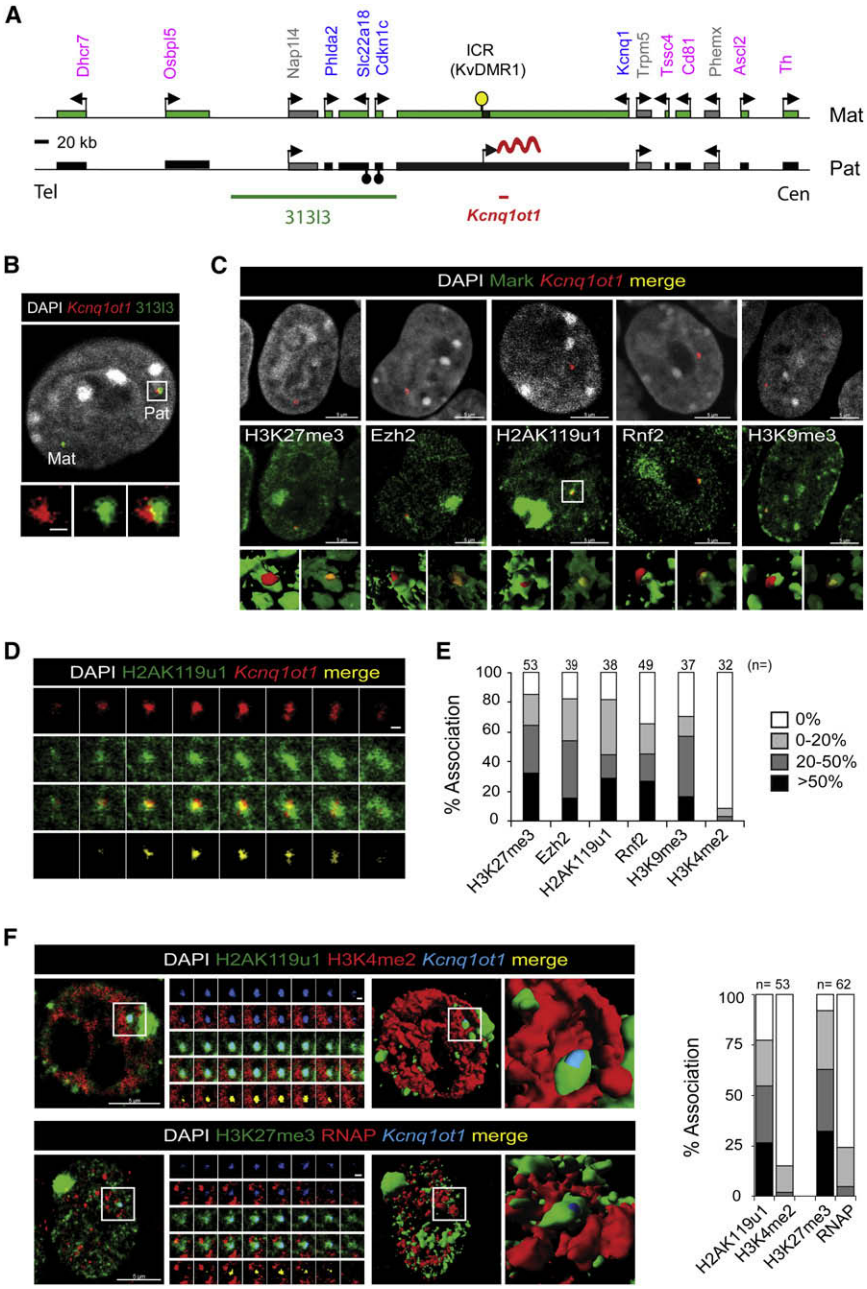

Figure 1. Nascent *Kcnq1ot1* ncRNA Marks a Distinct Subnuclear Repressive Compartment in TS Cells

(A) Schematic representation of the ~1 Mb mouse *Kcnq1* cluster with allelic transcription (arrows) as determined in placenta at E9.5/E13.5 (Schulz et al., 2006; Umlauf et al., 2004). *Kcnq1ot1* ncRNA is controlled by the *KvDMR1* ICR. Ubiquitously imprinted "inner" genes (blue), placental-specific imprinted "outer" genes (pink), and nonimprinted genes (gray) are indicated. Yellow and black lollipops indicate germline and somatic DNA methylation, respectively. Tel, telomeric; Cen, centromeric; Mat, maternal; Pat, paternal.

(B) RNA/DNA-FISH detection of *Kcnq1ot1* (red) and *Kcnq1* parental loci (313I3, green) in TS cells.

(C) Immuno-RNA-FISH for H3K27me3, Ezh2, H2AK119u1, Rnf2 and H3K9me3 (green), and *Kcnq1ot1* ncRNA (red) in female TS cells. Small bottom panels show 3D reconstructions (left) highlighting colocalization between *Kcnq1ot1* ncRNA and marks/proteins in yellow (right). The inactive X chromosome is also strongly enriched in PcG marks/proteins.

(D) Serial optical sections illustrating the 3D association of *Kcnq1ot1* (red) with a repressive compartment enriched in H2AK119u1 (green), insert from (C). Yellow indicates colocalization between RNA and H2AK119u1.

(E) Percentage of cells with different association levels between *Kcnq1ot1* and indicated marks/proteins. Serial confocal *z* slices were used for 3D reconstructions and quantifications. The occupancy level of the *Kcnq1ot1* signal with a chromatin mark is categorized as follows: high (>50%), intermediate (20%–50%), limited overlap (0%–20%), or exclusion of the mark from the domain defined by the ncRNA (0%). The number of nuclei analyzed is indicated.

(F) Double immunofluorescence detection of H2AK119u1 (green) and H3K4me2 (red) or of H3K27me3 (green) and RNAP (red), followed by *Kcnq1ot1* RNA-FISH (blue). Serial confocal *z* slices with colocalization between repressive marks and *Kcnq1ot1* (yellow) are shown. 3D-reconstructed views of nuclei and close-ups (right panels) illustrate exclusion of H3K4me2 and RNAP from the repressive paternal *Kcnq1* domain marked by *Kcnq1ot1*. Quantifications as in (E). Scale bars: 5 μm (nuclei) and 0.5 μm (magnifications).

Deficiency for the H3K9 histone methyltransferase *G9a* causes stochastic loss of imprinted repression of outer *cis* genes in placental tissues of E9.5 embryos (Wagschal et al., 2008), underscoring the importance of multiple repressive pathways in imprinted repression. Recent studies suggest that *Kcnq1ot1*-mediated silencing initiates during early embryonic development and is maintained along the entire the *Kcnq1* domain, exclusively in the extraembryonic lineages (Green et al., 2007; Lewis et al., 2006; Umlauf et al., 2004). However, the timing and nature of the chromatin features associated with the initiation of imprinted silencing have remained elusive.

In this manuscript, we characterize the higher-order chromatin and genomic organization at the paternal repressed *Kcnq1* cluster in preimplantation embryos and in trophectodermal stem (TS) cells, an in vitro model system for early extraembryonic development. By combining RNA-FISH with immunofluorescence staining and DNA-FISH, we reveal the existence of a repressive subnuclear compartment at the paternal *Kcnq1* and *Igf2r* clusters, as previously identified at the X_i (Okamoto et al., 2004). Importantly, we provide unprecedented in vivo evidence that, in comparison to the active maternal cluster, the paternally repressed *Kcnq1* cluster exists in a three-dimensionally (3D) contracted state in early embryos. In the absence of maternal and zygotic *Ezh2* expression and H3K27me3, the paternal *Kcnq1* repressive compartment remained largely intact. Yet, paternal genomic contraction was abrogated, and several *cis* genes failed to be

silenced in extraembryonic tissues after implantation. Remarkably, comparable observations were made in the absence of maternal and zygotic *Rnf2* expression. Our results indicate that during early development, the paternal *Kcnq1* cluster becomes progressively competent for silencing *cis* genes through the formation of a higher-order repressive compartment and PcG-mediated genomic reorganization.

RESULTS

The *Kcnq1ot1* and *Air* ncRNAs Distinguish Discrete Repressive Nuclear Compartments

To study whether the ~90 kb *Kcnq1ot1* ncRNA (Mohammad et al., 2008) directs the formation of a repressive nuclear compartment, we established a RNA-FISH assay in TS cells in which *Kcnq1ot1* is paternally expressed (Lewis et al., 2006). Using a probe intronic to *Kcnq1* and covering 11 kb of the *Kcnq1ot1* transcriptional region (Figure 1A), we detected a single, intense RNA-FISH signal in 90.6% (SD ±4.1%; n = 1050) of TS cells. By combining RNA and DNA-FISH, we observed that the *Kcnq1ot1* transcript originates from the *Kcnq1* locus on one parental chromosome (Figure 1B), confirming the specificity of *Kcnq1ot1* detection by RNA-FISH. Treatment of TS cells with the RNAP elongation inhibitor DRB led to a rapid and dramatic reduction in *Kcnq1ot1* levels by quantitative PCR and FISH (see Figure S1 available online), suggesting low transcript stability and continuous RNAP-dependent transcription of the *Kcnq1ot1* ncRNA.

Next, we combined immunodetection and RNA-FISH to investigate whether the *Kcnq1ot1* ncRNA associates with a repressive subnuclear domain at the paternal *Kcnq1* cluster in female TS cells. Remarkably, the analyses of consecutive confocal sections revealed strong enrichment for PcG proteins and Polycomb-mediated marks as well as H3K9 trimethylation (H3K9me3) at proximity to, and in association with, the *Kcnq1ot1* ncRNA signal (Figures 1C and 1D). To quantify the level of association, we generated 3D reconstructions of confocal stacks and determined the relative volume of the *Kcnq1ot1* domain that is labeled by a given chromatin mark (Figure 1C, bottom panels). For H3K27me3 and Ezh2, the PRC2 component catalyzing this mark, we scored high percentages of cells with strong (>50%) and intermediate (20%–50%) levels of association with *Kcnq1ot1* (Figure 1E). We observed similar degrees of association for H2AK119u1 and the E3-ubiquitin ligase Rnf2. Finally, *Kcnq1ot1* was also extensively associated with selected other PcG-proteins (PRC2 proteins Eed and Suz12, and PRC1 proteins Cbx2, Rybp, and Phc2) and additional histone marks (H3K9me2 and H4K20me1) (Figure S2). In contrast, double immuno-RNA-FISH stainings revealed that markers for transcriptional activity such as H3K4me2 and RNAP were excluded from *Kcnq1ot1* and its surrounding chromatin enriched in H2AK119u1 and H3K27me3 (Figure 1F). Importantly, the size of the repressive chromatin compartment generally exceeds that of the domain delineated by the *Kcnq1ot1* ncRNA, suggesting limited association of *Kcnq1ot1* ncRNA with the flanking regions of the *Kcnq1* cluster (see below). A similar repressive compartment was observed at the *Igf2r* imprinted gene cluster using a probe directed against the *Air* ncRNA (Figures S3A–S3D). Altogether, these data identify higher-order repressive compartments for the paternal *Kcnq1* and *Igf2r* clusters, analogous to what was previously described for the inactive X chromosome.

Differential Chromatin Configurations at Parental *Kcnq1* Imprinted Clusters

To control for the specificity of *Kcnq1ot1* association with repressive chromatin, we directly compared the chromatin configuration at the maternal and paternal *Kcnq1* genomic clusters in TS cells. In these experiments, we combined immunodetection and RNA FISH detection of *Kcnq1ot1* ncRNA and nascent transcripts for *Osbpl5* or *Cd81*, two maternally expressed *cis* genes within the *Kcnq1* cluster (Figure 1A), as well as for the unrelated *LaminB1* nascent transcript. Maternally, we observed an "active" chromatin configuration rich in H3K4me2 and RNAP and devoid of H3K27me3 and H2AK119u1 (Figures S4 and S5). In the same nuclei, a repressive chromatin configuration was detected at the paternal allele, at proximity to *Kcnq1ot1*. *LaminB1* nascent RNA was equally devoid of H3K27me3 and H2AK119u1 (Figure S5). To additionally test whether the association of repressive marks with the *Kcnq1ot1* FISH signal could be explained by random, nonspecific proximity to one of the numerous nuclear spots, we performed an in silico simulation (Noordermeer et al., 2008). We developed an algorithm to generate diffraction-limited, randomly positioned loci in 3D confocal stacks and scored only limited levels of association relative to H3K27me3 and H2AK119u1, two marks highly associated with *Kcnq1ot1* (Figure S5). Altogether these data underscore the specificity of the immuno-RNA-FISH assay and support the notion that the two parental *Kcnq1* clusters exist in different nuclear chromatin configurations within the same cell.

H2AK119u1 Is Enriched at Imprinted Genes in a Parental-Specific Manner

To investigate whether the immuno-RNA FISH results reflect the local enrichment of repressive marks along the paternal *Kcnq1* cluster, we performed allele-specific chromatin immunoprecipitation (ChIP) analyses in undifferentiated TS cells. We used polymorphisms between *Mus musculus* C57BL/6J and *Mus spretus* (SD7) to distinguish parental alleles. We observed a 2- to 6-fold enrichment of H2AK119u1 around transcriptional start sites of paternal versus maternal alleles for three *cis* genes (*Cdkn1c*, *Tssc4*, and *Cd81*) (Figures 2A and 2B). Likewise, paternal alleles were also strongly enriched in H3K27me3, whereas maternal alleles were enriched in H3K4me2 and RNAP. At the *Osbpl5* locus, H2AK119u1 and H3K27me3 were about 2-fold enriched paternally. Parental enrichments were concordant with levels of allelic gene expression as analyzed by quantitative polymorphic RT-PCR (see Figures 7A–7C). In contrast, we observed no differential allelic enrichment at *Nap1l4*, a nonimprinted gene located within the *Kcnq1* cluster, underscoring the specificity of the ChIP conditions. As anticipated, RNAP and H3K4me2 were enriched at *KvDMR1*. This latter finding is in concordance with immuno-RNA-FISH results showing partial focal colocalization of *Kcnq1ot1* with RNAP (see Figure S4E), possibly marking the site of *Kcnq1ot1* transcription within the repressive compartment. Quantitative PCR analyses demonstrated comparable

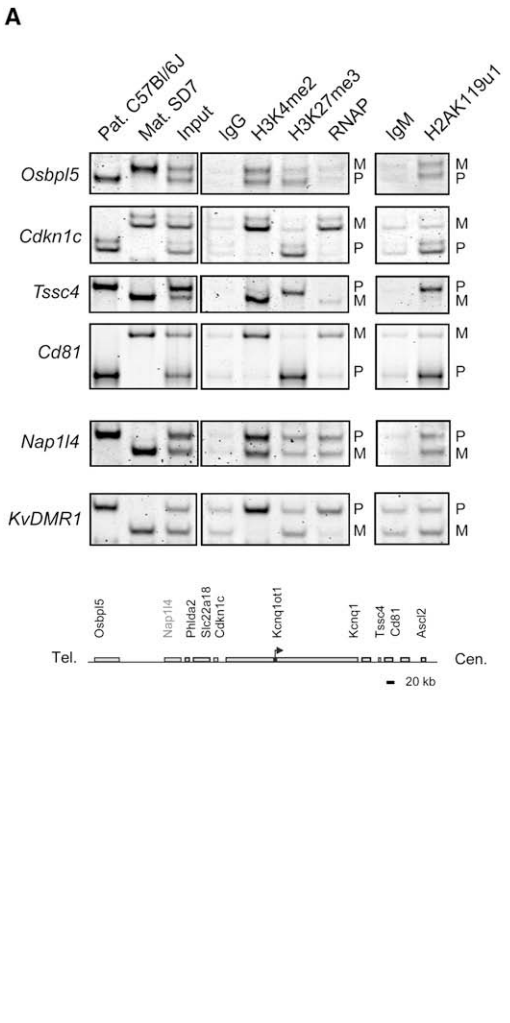

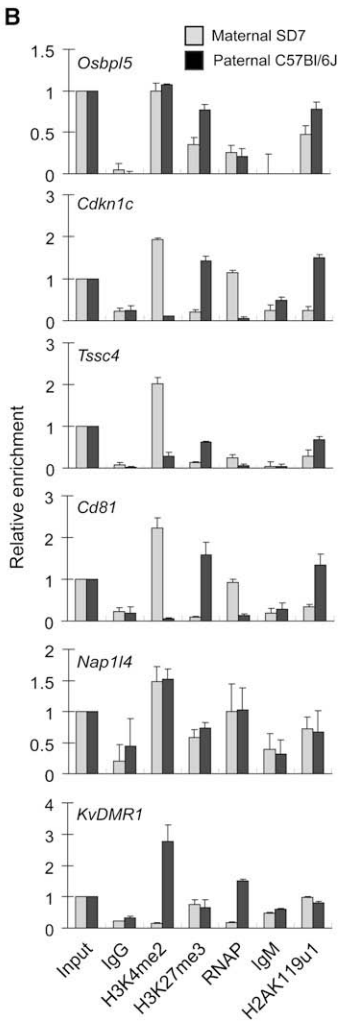

Figure 2. PRC1-Mediated H2AK119u1 Is Enriched at *Kcnq1* Imprinted Cluster *cis* Genes in TS Cells

(A) Allelic ChIP assays were carried out using antibodies directed against H2AK119u1, H3K4me2, H3K27me3, and RNAP. ChIP material was amplified by PCR, and parental alleles of *Cdkn1c*, *Tssc4*, *Cd81*, and *Osbpl5*, nonimprinted *Nap1l4*, and ICR *KvDMR1* were distinguished by SSCP. Results are representative of three independent ChIP experiments. M, maternal; P, paternal.

(B) Quantification of relative ChIP enrichment of assayed marks at the *Kcnq1* parental alleles shown in panel (A), normalized to input. Standard deviation was calculated from 2–3 PCR-SSCP gel repeats.

enrichments of H2AK119u1, H3K27me3, H3K4me2, and RNAP at imprinted versus nonimprinted control genes such as *HoxA9* and *Oct4* (Figure S6). Our ChIP results confirm allelic enrichment for repressive marks observed by immuno-RNA-FISH and, to our knowledge, demonstrate for the first time allele-specific enrichment of H2AK119u1 at repressed *Kcnq1* cluster *cis* genes. Taken together, our data strongly suggest a regulatory role not only for PRC2, but also for PRC1, in imprinted gene silencing.

In Vivo Dynamics of the "*Kcnq1* Compartment"

We next studied preimplantation embryos to address whether the imprinted repressive compartments exists in vivo. Remarkably, by FISH and PCR, we found *Kcnq1ot1* already expressed in mid- to late zygotes (at pronuclear stage 4–5) (Figures 3A–3C, data not shown), before the main wave of genome activation at the two-cell stage. As in TS cells, brief exposure of zygotes to the RNAP inhibitor DRB abrogated detection of *Kcnq1ot1* in the paternal pronucleus (Figure S1), demonstrating that the *Kcnq1ot1* ncRNA is instable and continuously transcribed in early embryos as well.

Immuno-RNA-FISH analyses revealed that the *Kcnq1ot1* ncRNA domain starts to associate with PRC2 (H3K27me3, Ezh2) and PRC1 (Rnf2) markers in zygotes (Figure 3). Levels of association were low in zygotes; they increased in two-cell embryos and remained high in trophectoderm cells (TE) of blastocyst embryos. Likewise, we consistently observed *Air* ncRNA expression and association with H3K27me3 in TE cells of blastocysts (Figure S3E), though not in zygotes (n = 26). Our results indicate an early establishment of the *Kcnq1ot1*-associated repressive domain during preimplantation embryonic development.

The *Kcnq1* Repressive Compartment Exists in the Absence of Ezh2 In Vivo

To investigate the function of PRC2 in the formation of the repressive compartment and initiation of imprinted repression, we generated embryos deficient for maternal and zygotic *Ezh2* expression ($Ezh2^{m-z-}$). In such embryos, Ezh2 proteins and global H3K27me3 are absent from the zygotic stage onward (Figure 4A) (Puschendorf et al., 2008). Nevertheless, $Ezh2^{m-z-}$ embryos develop normally to the blastocyst stage, at which we observed no change in cell number or in expression patterns of Oct4 and Cdx2, markers of the inner cell mass and trophectoderm (data not shown). We did not observe H3K27me3 staining in association with *Kcnq1ot1* nor with the X_i, marked by the *Xist* ncRNA, in female $Ezh2^{m-z-}$ embryos lacking the Ezh2 protein (Figure S7). Nevertheless, RNAP and active marks such as H3K4me2 and H3K36me3 were largely excluded from the *Kcnq1ot1* ncRNA domain in $Ezh2^{m-z-}$ as in wild-type (WT) blastocysts (Figures 4B and 4D, data not shown). Moreover, we measured similar levels of higher-order association for several PRC1 members (Rnf2, Cbx2, and Rybp) with *Kcnq1ot1* in both genotypes (Figures 4C and 4D and Figure S7). Altogether, these data confirm the catalytic inactivity of the PRC2 complex in the absence of Ezh2 and support PRC2-independent targeting of PRC1 members to the paternal *Kncq1* compartment. Importantly, maternal and zygotic Ezh2 function is not required for formation of the repressive compartment devoid of active marks and RNAP at the paternal *Kcnq1* cluster in vivo.

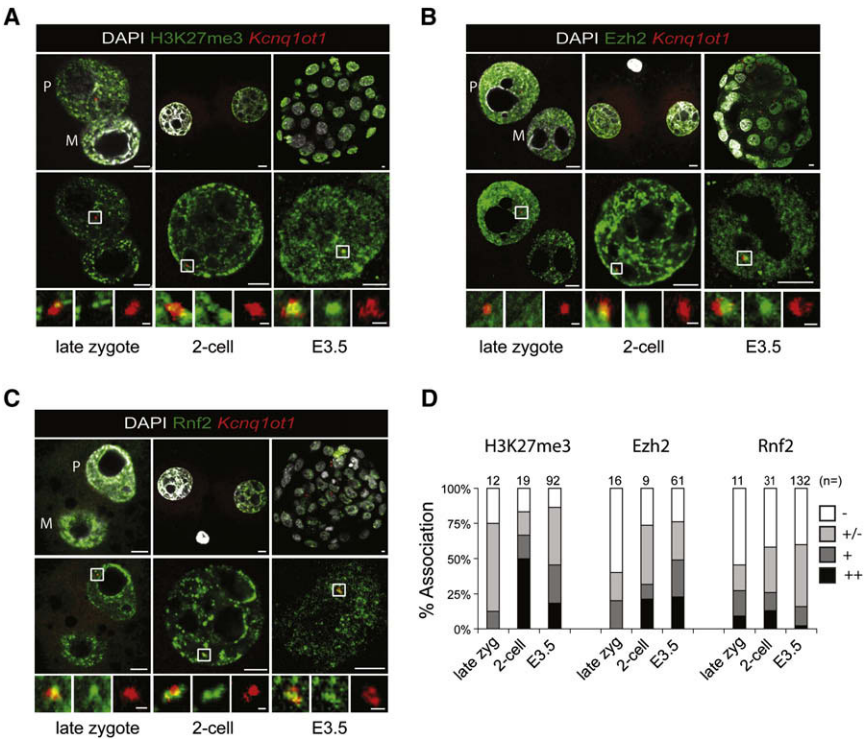

Figure 3. The *Kcnq1ot1*-Associated Repressive Configuration Is Established Early in Preimplantation Embryos

(A–C) Immuno-RNA-FISH for H3K27me3 (A), Ezh2 (B), and Rnf2 (C) (green) and *Kcnq1ot1* ncRNA (red) in preimplantation mouse embryos. Scale bars: 5 μm (embryos, nuclei) and 0.5 μm (magnifications).

(D) Scoring data indicating the percentage of cells with *Kcnq1ot1*/mark association at different stages of embryonic development (late zygote, two-cell stage, and blastocyst [E3.5] embryos). Quantifications were based on evaluating multiple serial 2D optical slices (described in Figure S2): high (++); intermediate (+); partial overlapping (+/−); exclusion of the mark from the domain defined by the ncRNA (−). The number of nuclei analyzed is indicated.

Ezh2 Regulates *Kcnq1ot1* ncRNA Association along the *Kcnq1* Genomic Cluster

In human cell lines, *KCNQ1OT1* has been reported to physically interact with inner *cis* genes (*CDKN1C* and *SLC22A18*) within the *KCNQ1* cluster (Murakami et al., 2007). To assess the extent of interaction of *Kcnq1ot1* along the *Kcnq1* cluster, we combined RNA-FISH for *Kcnq1ot1* and DNA-FISH for distinct regions of the *Kcnq1* genomic cluster. Codetection of *Kcnq1ot1* and a probe telomeric to the *Kcnq1* gene (313I3) in TS cells revealed only partial overlap between the RNA and genomic region (see Figure 1B and Figure 4F, left panel), suggesting limited spreading of the ncRNA in *cis*. To extend these analyses to more distant genomic regions and to evaluate the regulatory role of *Ezh2* in such interactions in vivo, we used two differentially labeled BAC probes, specific for the centromeric (473N24) and telomeric (16K9) ends of the *Kcnq1* cluster on WT and $Ezh2^{m-z-}$ blastocysts (Figure 4E). In each trophectodermal cell, we determined the relative volume of the DNA-FISH signals that is also occupied by the *Kcnq1ot1* ncRNA signal. In WT blastocysts, *Kcnq1ot1* partially colocalized with 473N24 and 16K9 genomic regions, confirming limited coating of the *Kcnq1ot1* ncRNA along the *Kcnq1* cluster. Interestingly, in $Ezh2^{m-z-}$ embryos, colocalization levels were significantly reduced for both regions, with a majority of nuclei showing no physical association between *Kcnq1ot1* and 16K9 or 473N24 (Figure 4F, illustrated in Figure 4E). However, no difference in the levels of *Kcnq1ot1* RNA was detected by RNA-FISH in WT and $Ezh2^{m-z-}$ embryos (data not shown). These data thus suggest an important function for Ezh2 in either spreading of the *Kcnq1ot1* ncRNA along the imprinted gene cluster in *cis* and/or in organizing the three-dimensional genomic organization of the cluster.

Ezh2 Mediates Genomic Contraction In Vivo

To address the latter possibility, we directly compared the genomic organization of the two parental *Kcnq1* imprinted gene clusters in WT and $Ezh2^{m-z-}$ conditions. We performed RNA/DNA-FISH as described above and measured the physical distance between the centroids of the FISH signals detected by the 16K9 and 473N24 BAC probes (Figure 4E). We identified the paternal alleles on the basis of *Kcnq1ot1* expression. After normalization to the nuclear radius, we revealed significantly shorter distances between the two FISH signals at paternal over maternal *Kcnq1* genomic clusters in WT TS cells (exact Wilcoxon Mann-Whitney rank sum test; n = 94; $p = 6.9 \times 10^{-6}$) (Figures 5A and 5B). We did not find evidence for significant parental-specific *Kcnq1* association with pericentric heterochromatin nor with nuclear periphery (Figures S8A and S8B), two compartments that have been associated with gene silencing in several cell differentiation systems (Brown et al., 1997; Wiblin et al., 2005). These data suggest that the paternal *Kcnq1* imprint cluster constitutes an autonomous repressive nuclear compartment in TS cells, characterized by a contracted genomic state.

To assay whether a similar local organization exists in vivo, we repeated the analyses in TE cells of WT and $Ezh2^{m-z-}$ blastocysts. In WT embryos, we observed a significantly higher degree of contraction at the paternal imprinted versus the maternal nonimprinted gene cluster (n = 112; $p = 4.8 \times 10^{-5}$) (Figures 5C and 5D). Remarkably, in $Ezh2^{m-z-}$ embryos, the median and distribution of intercentroid distances were equivalent between the paternal and maternal alleles (n = 93; p = 0.25) (Figures 5E and 5F). Direct comparison of alleles in WT and mutant embryos showed that in $Ezh2^{m-z-}$ blastocysts the paternal allele exists in a relaxed configuration, comparable to the configuration of maternal alleles in both genotypes (Figure S8C). Furthermore, we observed no difference in nuclear radius between WT and $Ezh2^{m-z-}$ trophectodermal cells (Figure S8D). Pair-wise parental comparison of the *Kcnq1* cluster organization in single nuclei demonstrated that the paternal genomic *Kcnq1* cluster is more contracted than its

maternal counterpart in 70% of WT trophectodermal cells (Figure 5G, top panel), confirming differential organization of parental imprinted gene clusters in blastocyst embryos. In contrast, in the absence of Ezh2 we observed a random distribution of parental genomic organization, with 50% of nuclei displaying paternal contraction.

To test whether genomic contraction of the paternal *Kcnq1* cluster is maintained during implantation, we performed contraction analyses on extraembryonic ectodermal (Eee) cells carefully dissected from embryos isolated at embryonic day (E) 6.5 of gestation. As in the E3.5 TE cells, we measured a high level of contraction of the paternal imprinted cluster in WT E6.5 postimplantation Eee cells ($n = 47$; $p = 1.6 \times 10^{-5}$) (Figure 5H). In the absence of maternal and zygotic *Ezh2* expression, however, genomic contraction was alleviated ($n = 53$; $p = 0.15$) (Figures 5H and 5G). Taken together, our data demonstrate that Ezh2 is required for higher-order genomic contraction of the paternal *Kcnq1* cluster in extraembryonic lineages in vivo. Genomic contraction initiates during preimplantation development and is maintained in subsequent stages of development.

The E3-Ubiquitin Ligase Rnf2 Is also Required for *Kcnq1* Genomic Contraction In Vivo

Besides Ezh2, our FISH and ChIP data strongly suggest a regulatory role for the PRC1 complex and H2AK119 monoubiquitination in imprinted gene silencing (Figures 1, 2, and 3). To test the relative contributions of PRC2 and PRC1 in regulating *Kcnq1* imprinting, we generated embryos deficient for maternal and zygotic *Rnf2* expression ($Rnf2^{m-z-}$). In such embryos, the PRC1 complex was disrupted, and proteins such as Bmi1 and Phc2 were undetectable from the zygotic stage onward (Puschendorf et al., 2008) (Figure S9). Nevertheless, $Rnf2^{m-z-}$ embryos developed normally to the blastocyst stage and up to 6.5 days of embryonic development. Importantly, in $Rnf2^{m-z-}$ E3.5 TE cells, the *Kcnq1ot1*-associated repressive compartment was maintained, as assayed by the presence of PRC2-mediated H3K27me3 and absence of RNAP (Figures 6A and 6B). We next investigated the requirement for Rnf2 in *Kcnq1* genomic organization and observed loss of paternal contraction ($n = 42$; $p = 0.37$) (Figure 6C and Figure S10), indicating that Rnf2 and, by extension, the PRC1 complex, is also required for organizing the paternal *Kcnq1* cluster in vivo.

PcG Proteins Ezh2 and Rnf2 Regulate Imprinted Repression In Vivo

We next investigated the role of PcG proteins Ezh2 and Rnf2 in initiating imprinted silencing at the paternal *Kcnq1* cluster during early embryonic development. To distinguish between parental alleles, we generated control ($Ezh2^{F/F}$ and $Rnf2^{F/F}$) and PcG mutant ($Ezh2^{m-z-}$ and $Rnf2^{m-z-}$) embryos heterozygous for *Mus musculus* and *Mus spretus* (SD7) along the *Kcnq1* cluster. We first analyzed the imprinting status in E3.5 control embryos. Using semiquantitative allelic RT-PCR analyses (Umlauf et al., 2004) and as previously reported (Lewis et al., 2006), we found biallelic expression with a maternal bias for three genes (*Cdkn1c*, *Tssc4*, and *Cd81*), but not for *Osbpl5*. In $Ezh2^{m-z-}$ E3.5 embryos, gene expression patterns were not affected (Figures 7A and 7B).

In WT E6.5 postimplantation embryos, the inner *Cdkn1c cis* gene was monoallelicaly expressed from the maternal allele in both embryonic and extraembryonic tissues (Figure 7A). In contrast, the outer *cis* genes *Tssc4* and *Cd81* showed monoallelic repression only in extraembryonic tissues, while *Osbpl5* was found expressed from both parental alleles with a maternal bias in tissues of both lineages. In $Ezh2^{m-z-}$ E6.5 embryos, imprinted repression of *Cdkn1c*, *Tssc4*, and *Cd81* was strongly impaired, exclusively in extraembryonic tissues (Eee). No significant change in allelic repression was noticed for *Osbpl5*, and this may relate to the lower degree of imprinted paternal repression observed in WT tissues at this stage of development.

To quantify the changes in paternal gene expression in the absence of Ezh2, we developed sets of real-time primers that selectively amplify either *Mus musculus* or *Mus Spretus* alleles (Figure 7C, controls). Using this quantitative method, we recapitulated all results obtained in the above-mentioned analyses. We measured 3- to 100-fold increased levels of expression along the paternal domain, exclusively in the extraembryonic tissue of E6.5 $Ezh2^{m-z-}$ embryos (Figure 7C, paternal). These data strongly support a role for Ezh2 in imprinted repression along the entire paternal *Kcnq1* cluster. Remarkably, while no change in gene expression was visible for the maternal *Cd81* and *Tssc4* loci, we observed an 8-fold change in expression for the maternal allele of the inner gene *Cdkn1c* (Figure 7C, maternal).

We next investigated the imprinting status in $Rnf2^{m-z-}$ E6.5 embryos. To our surprise, the lack of Rnf2 phenocopied the expression changes observed in $Ezh2^{m-z-}$ extraembryonic tissues (Figure 7C, paternal). Noticeably, maternal and paternal *Cdkn1c* expression levels were also upregulated in embryonic tissues in the absence of Rnf2 expression (Figure 7C). Quantitative analyses also confirmed the nonimprinted status of *Osbpl5* (Figure 7C). The expression of *Osbpl5* was increased both maternally and paternally in the absence of both Ezh2 and Rnf2, but the relative parental expression ratios were conserved, suggestive of an imprinting-independent loss of silencing (rather than loss of imprinting), at least at this stage of development.

In summary, our data demonstrate that the PcG proteins Ezh2 and Rnf2 function in parallel to mediate full allelic repression at inner (*Cdkn1c*) and outer (*Cd81*, *Tssc4*) *cis* genes within the *Kcnq1* cluster in extraembryonic tissues. We also provide evidence for Rnf2 having a role in imprinted silencing of *Cdkn1c* in the embryo proper. Our data finally suggest differential, position-dependent regulation of the *Kcnq1*-domain genes, both on the paternal and the maternal alleles.

DISCUSSION

Here, we demonstrate that the paternal *Kcnq1* imprinting cluster organizes a distinct higher-order repressive nuclear compartment in TS cells and early embryos. The "*Kcnq1* chromatin compartment" is characterized by the local presence of *Kcnq1ot1* transcripts, association of PRC2 and PRC1 proteins, and of various repressive histone modifications, and by exclusion of RNAP and active histone modifications. By ChIP, we confirm local enrichment of H2AK119u1 and H3K27me3 at repressed paternal alleles devoid of H3K4me2 and RNAP. During development, *Kcnq1ot1* is continuously expressed from the paternal *Kcnq1* locus from the zygote stage onward. Catalytically active PRC1 and PRC2 complexes rapidly localize at proximity to the *Kcnq1ot1* nascent transcripts and show high levels of association in

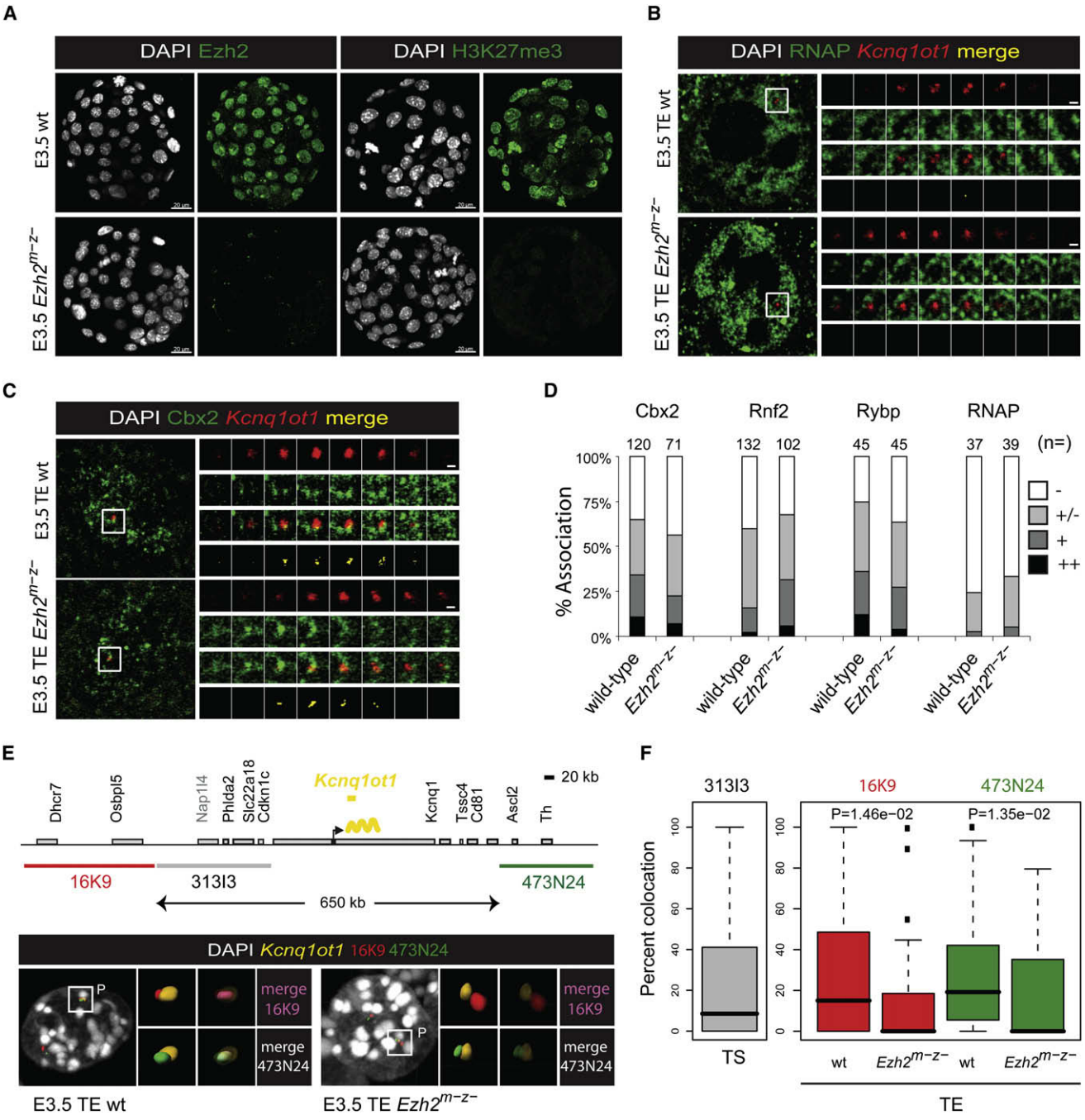

Figure 4. Ezh2 Is Dispensable for the Formation of the Paternal *Kcnq1* Repressive Compartment

(A) Immunostaining for Ezh2 and H3K27me3 (green) showing global loss of Ezh2 and H3K27me3 in *Ezh2*$^{m-z-}$ blastocysts.

(B) Immuno-RNA-FISH for RNAP (green) and *Kcnq1ot1* (red) showing normal exclusion of the transcription machinery from the repressive *Kcnq1* compartment in WT and *Ezh2*$^{m-z-}$ trophoblast cells (TE).

(C) Immuno-RNA-FISH for Cbx2 (green) and *Kcnq1ot1* (red) indicating normal higher-order association of this PRC1 protein with the *Kcnq1ot1* ncRNA domain in *Ezh2*$^{m-z-}$ E3.5 TE cells. Serial *z* slices with the colocalization channel (yellow) illustrate the extent of association/exclusion of the Cbx2 and RNAP with/from *Kcnq1ot1*. Scale bar of magnifications: 0.5 μm.

(D) Quantification of the association of *Kcnq1ot1* to RNAP and PRC1-member proteins in WT and *Ezh2*$^{m-z-}$ embryos. The number of nuclei analyzed is indicated. Rnf2 data in WT cells are identical to those in Figure 3D.

(E) Schematic diagram showing the genomic position of BACs used to detect the flanking regions of the genomic *Kcnq1* cluster. *Kcnq1ot1* RNA-FISH (yellow) marks the paternal *Kcnq1* cluster. 3D RNA/DNA-FISH detection of the *Kcnq1* parental loci in WT and *Ezh2*$^{m-z-}$ E3.5 TE cells. 3D reconstructions show both parental loci (left panel). Overlap between BAC-16K9 (red) or BAC-473N24 (green) with *Kcnq1ot1* ncRNA signal (yellow) was measured using new colocalization channels (right panels: merge 16K9/*Kcnq1ot1* indicated in pink; merge 473N24/*Kcnq1ot1* indicated in white). P, paternal.

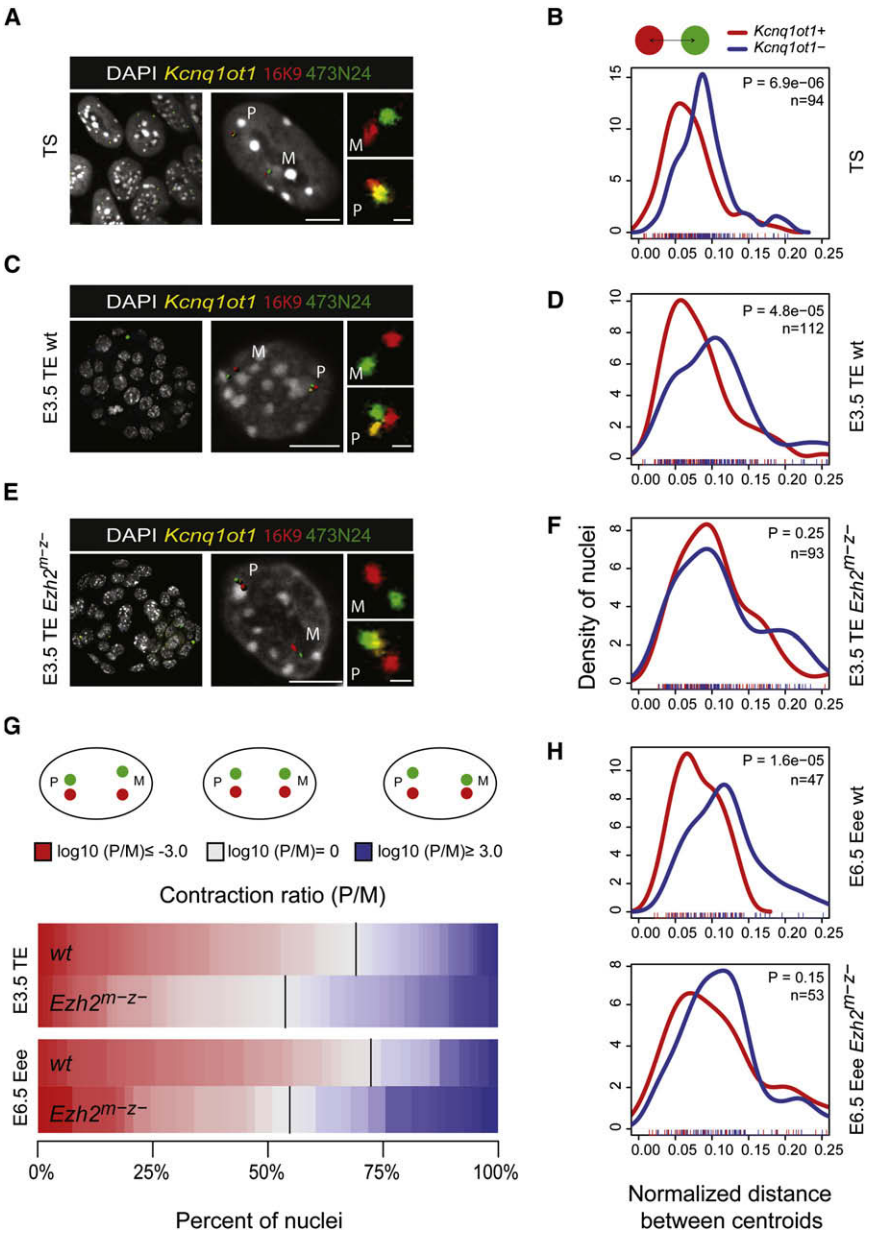

Figure 5. *Ezh2*-Dependent Genomic Contraction of the Paternal *Kcnq1* Imprinted Gene Cluster In Vivo

(A, C, and E) 3D RNA/DNA-FISH detection of the *Kcnq1* parental loci in TS cells and WT and *Ezh2*$^{m-z-}$ E3.5 TE cells. The distance between centroids of 16K9 (red) and 473N24 (green) DNA-FISH signals was measured to evaluate the degree of compaction at the parental *Kcnq1* genomic clusters. 3D reconstructions show both parental loci (middle panel). Single optical sections illustrate the extent of contraction at parental alleles (right panels). Scale bars: 5 μm (nuclei) and 0.5 μm (magnifications). M, maternal, P, paternal.

(B, D, and F) Distributions of intercentroid distances of FISH signals at paternal (*Kcnq1ot1*+, red) and maternal alleles (*Kcnq1ot1*−, blue) in WT TS cells (B) and WT and *Ezh2*$^{m-z-}$ E3.5 TE cells (D and F). Measurements were normalized to the radius of individual nuclei. p values indicate statistical significance of differences in distances measured at paternal and maternal alleles.

(G) Pair-wise parental contraction ratios (P/M) in WT and *Ezh2*$^{m-z-}$ E3.5 TE cells were mapped to colors by sorting, taking their base-ten logarithm, and assigning them linearly to colors ranging from red (log10 (P/M) ≤ -3.0) over gray (log10 (P/M) = 0, indicated by a black line) to blue (log10 (P/M) ≥ 3.0). Schematic representations illustrate genomic organization of parental loci (top).

(H) Distributions of intercentroid distances of FISH signals at paternal (*Kcnq1ot1*+, red) and maternal alleles (*Kcnq1ot1*−, blue) in WT and *Ezh2*$^{m-z-}$ extraembryonic ectoderm (Eee) cells.

two-cell stage embryos (Figure 7C). A similar repressive compartment exists at the *Igf2r* imprinting cluster. In analogy to *Xist* (Chaumeil et al., 2006), these data point toward a direct role of the *Kcnq1ot1* and *Air* long ncRNAs in mediating gene silencing in *cis*, by nucleating repressive subnuclear compartments devoid of the transcriptional machinery, prior to actual silencing of *cis* genes (reviewed in Pauler et al., 2007; Umlauf et al., 2008). The low stability of the *Kcnq1ot1* ncRNA (Figure S1), its limited association along the *Kcnq1* genomic cluster (Figure 4), and the incomplete overlap between the ncRNA and the different repressive marks (Figures 1, 3, and 4, and Figure S2) indicate, however, that the mechanistic role of the nascent ncRNAs in imprinted silencing would be dynamic and spatially restricted. Developmentally, the *Kcnq1ot1* transcripts may be required continuously or only transiently. Given the existence of many noncoding transcripts in mammals (Katayama et al., 2005), some of the many Polycomb-repressive nuclear compartments we observed in TS cells and early embryos may represent other sites of ncRNA-mediated silencing (Rinn et al., 2007).

Within the *Kcnq1* cluster, the level of imprinted repression varies among genes and between embryonic and extraembryonic tissues at E6.5 of gestation. In blastocysts, *Cdkn1c*, *Tssc4*, and *Cd81* are partially imprinted (Lewis et al., 2006; Umlauf et al., 2004). We propose that imprinted repression is progressively established, starting during preimplantation

(F) Quantification of overlap as a percentage of the DNA-FISH signal volume occupied by the *Kcnq1ot1* ncRNA signal volume in WT and *Ezh2*$^{m-z-}$ E3.5 TE cells. The overlap of BAC-313I3 and *Kcnq1ot1* in TS cells is plotted on the left panel. In box plots, solid line, box hinges, and whiskers indicate median, quartile, and extreme values. Outliers, defined as values deviating more than 1.5 times the interquartile range from the closest quartile, are plotted individually as rectangles. p values indicate statistical significance of differences in overlap measured in WT (n = 34) and *Ezh2*$^{m-z-}$ (n = 30) E3.5 TE cells.

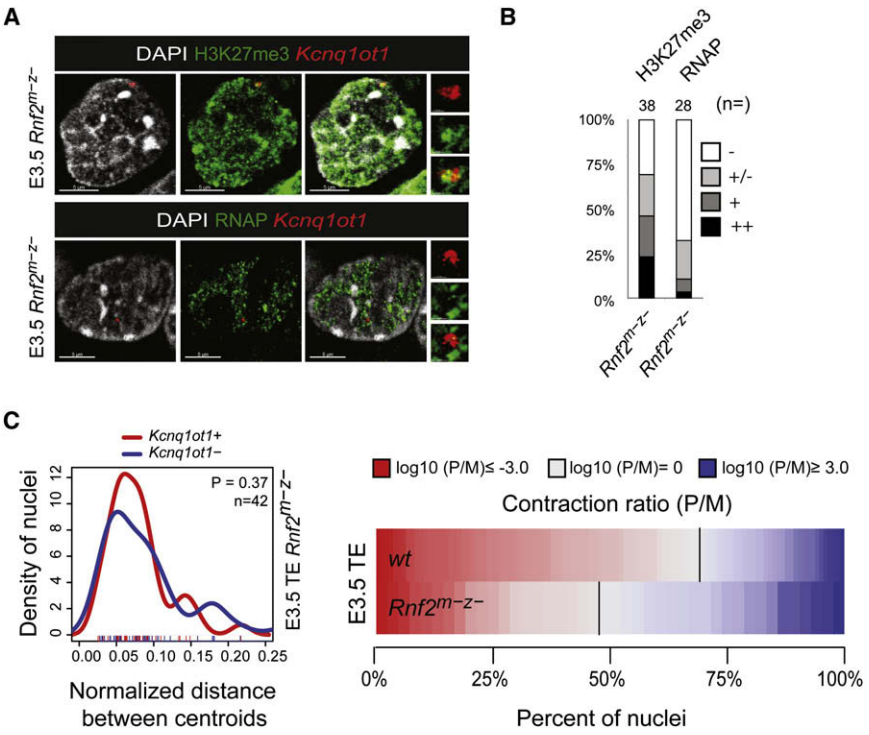

Figure 6. *Rnf2*-Dependent Genomic Contraction of the Paternal *Kcnq1* Imprinted Gene Cluster In Vivo

(A and B) Immuno-RNA-FISH for H3K27me3 and RNAP (green) and *Kcnq1ot1* (red) indicate normal higher-order association of H3K27me3 and exclusion of the transcription machinery from the repressive *Kcnq1* compartment in the absence of maternal and paternal Rnf2 ($Rnf2^{m-z-}$) TE cells. The number of nuclei analyzed is indicated.

(C) Distributions of intercentroid distances of FISH signals at paternal (*Kcnq1ot1*+, red) and maternal alleles (*Kcnq1ot1*−, blue) in $Rnf2^{m-z-}$ E3.5 TE cells (left). Measurements were normalized to the radius of individual nuclei. Pair-wise parental contraction ratios (P/M) in WT and $Rnf2^{m-z-}$ E3.5 TE cells.

development and continuing through peri-implantation stages in a gene- and lineage-specific manner. Akin to the recruitment of genes into the *Xist* domain during the course of random X chromosome inactivation, as characterized in differentiating ES cells (Chaumeil et al., 2006), physical relocalization of *cis* genes into the *Kcnq1* repressive compartment devoid of RNAP, likely controlled by Polycomb group complexes (see below), may be required for full imprinted repression in vivo. The observed developmental delay in imprinted repression versus early formation of the repressive contracted compartment may thus be due to constraints initially limiting the association of *cis* genes with the *Kcnq1* repressive domain.

Our loss-of-function analyses in postimplantation embryos show that Ezh2 and Rnf2 are equally required in extraembryonic tissues to mediate full repression at inner and outer *cis* genes. As observed for Rnf2 at the X_i (Schoeftner et al., 2006), but in contrast to developmental regulatory genes (Boyer et al., 2006), targeting of PRC1 components to the *Kcnq1* repressive compartment is independent of PRC2 function, at least at the higher-order level. We also find the targeting of PRC2-mediated H3K27me3 to be independent of Rnf2. Besides the PcG pathways, imprinting along the *Kcnq1* cluster is also regulated by H3K9 methylation (Wagschal et al., 2008). We propose that multiple layers of partially redundant, possibly synergistic, repressive pathways regulate imprinted gene silencing at the *Kcnq1* cluster during development. Their relative contribution and synergies in time remain to be elucidated. For *Cdkn1c*, partial loss of paternal repression was previously reported in *Eed*-deficient E7.5 whole embryos (Mager et al., 2003). Our quantitative results indicate that this reported loss of imprinting is largely due to abrogated paternal silencing in the extraembryonic rather than embryonic lineage. Silencing of *Cdkn1c* in E6.5 embryonic tissues was reported to depend on a repression mechanism that functions through the *KvDMR1* locus but independently of *Kcnq1ot1* transcription and DNA methylation (Shin et al., 2008). We identify Rnf2 as a regulator of *Cdkn1c* imprinting in the embryonic lineage, suggesting a repressive role for H2AK119u1, prior to the recruitment of DNA methylation to the *Cdkn1c* promoter at later stages of development. Collectively, our observations indicate the existence of multiple and stepwise-acting repressive mechanisms involved in initiating repression at paternal *Kcnq1* cluster.

In wild-type trophectodermal cells of blastocysts and TS cells, physical distances between the proximal and distal ends of *Kcnq1* clusters were on average two times shorter at paternal versus maternal *Kcnq1* clusters. Hence, we identify genomic contraction as an early feature of the imprinted repressed state. Genomic contraction presumably reflects a condensed spatial configuration (Lanzuolo et al., 2007) formed either through looping and/or local chromatin compaction of specific genomic regions within the *Kcnq1* cluster.

Loss of contraction in $Ezh2^{m-z-}$ and $Rnf2^{m-z-}$ embryos defines both PRC complexes as master regulators of higher-order genomic organization at the *Kcnq1* imprinted cluster. Intriguingly, *Kcnq1ot1* contains a short repeat motif required for gene silencing in *cis* (Mohammad et al., 2008). Likewise, *Xist* harbors A-rich repeats required for gene silencing and for targeting of *cis* genes into the repressive compartment of the X_i (Chaumeil et al., 2006). Since the association of *Kcnq1ot1* to proximal and distal regions of the *Kcnq1* cluster is significantly reduced in $Ezh2^{m-z-}$ embryos, we hypothesize that contraction is required for stable and complete silencing by facilitating targeting of *cis* genes, possibly directly via sequence elements in *Kcnq1ot1*, into the repressive compartment lacking the transcriptional machinery. Genomic contraction may also contribute to local targeting of various repressive modifications at regulatory elements of *cis* genes. Locus contraction and decontraction play crucial roles in *Igh* and *Tcr* recombination

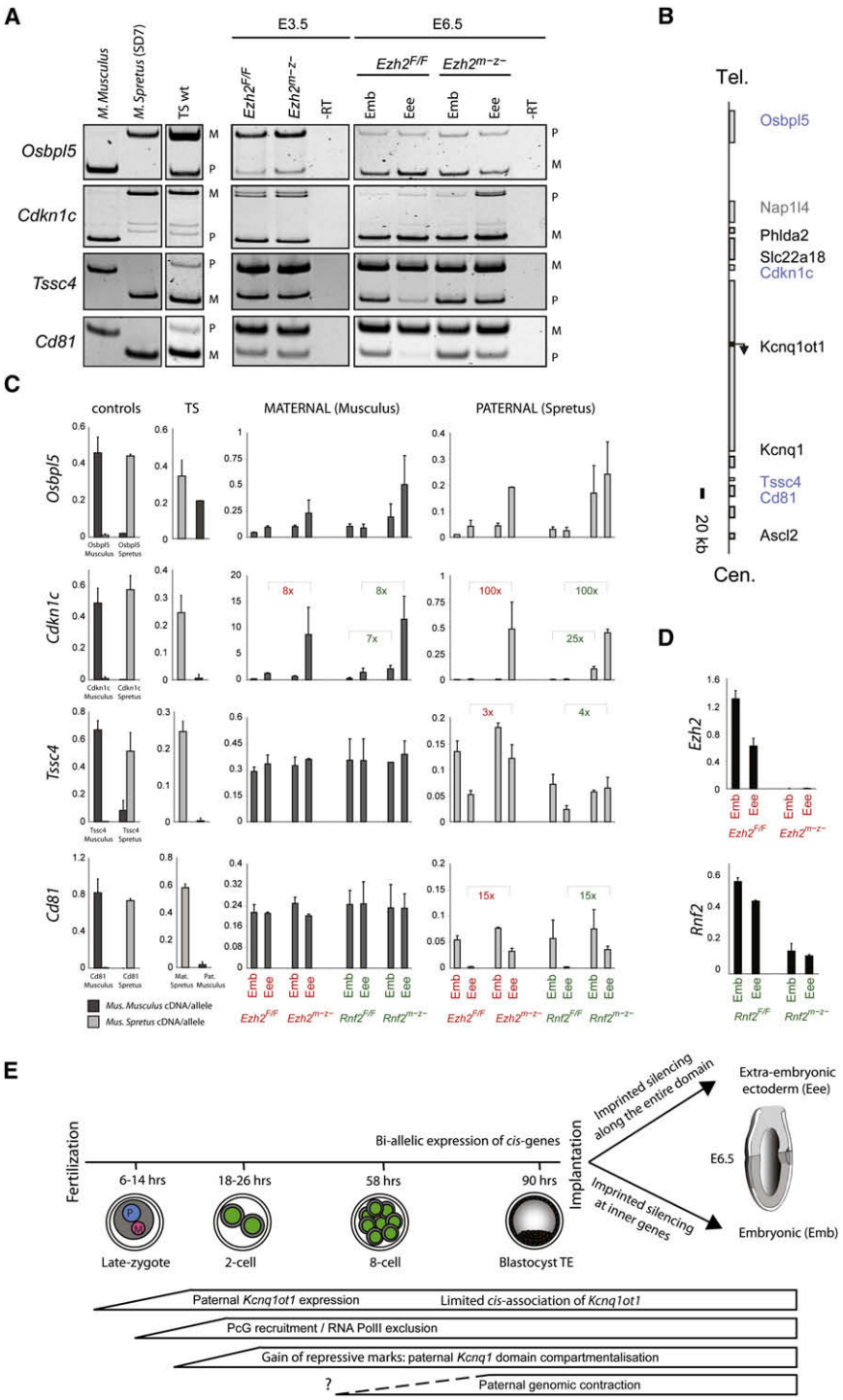

Figure 7. *Ezh2* and *Rnf2* Direct Monoallelic Silencing of *Kcnq1* Cluster *cis* Genes in Extraembryonic Tissues

(A) Allele-specific RT-PCR analyses of *Kcnq1* cluster *cis* genes (inner *Cdkn1c*; outer *Cd81*, *Tssc4*, and *Osbpl5*) in WT and $Ezh2^{m-z-}$ E3.5 embryos and E6.5 embryonic (Emb) and extraembryonic ectoderm (Eee) tissues (maternal C57BL/6J, paternal SD7). TS cell RNA from a reverse genetic cross was used to control for primer bias. Reverse transcription in the absence of reverse transcriptase (−RT) controls for specificity of cDNA amplification. Identical observations were made from 5–8 independent pools of embryos/tissues. M, maternal, P, paternal.

(B) Schematic diagram of *Kcnq1* imprinted cluster with studied genes highlighted in blue.

(C) Allele-specific RT-PCR analyses of *Kcnq1* cluster *cis* genes in control and PcG (*Ezh2* and *Rnf2*) mutant E6.5 Emb and Eee tissues. Control panels illustrate the species-specificity of primers used in these analyses. Relative maternal and paternal *Kcnq1 cis* gene expression levels were measured, and fold changes of paternally imprinted genes (*Cdkn1c*, *Tssc4*, and *Cd81*) are indicated. TS cells from a reverse cross were used as above. Data were normalized to *Gapdh* and to *Cytochrome1* expression levels, and standard deviations were calculated from three independent biological replicates.

(D) Quantitative expression levels of *Ezh2* and *Rnf2* in WT and mutant E6.5 samples.

(E) A working model: From the late-zygote stage onward, the paternal *Kcnq1ot1* ncRNA is continuously transcribed and mediates, directly or indirectly, the formation of a repressive chromatin compartment devoid of the transcriptional machinery. In blastocysts and postimplantation embryos, the paternal imprinted gene cluster exists in a contracted state. Genomic contraction and full paternal silencing of *Kcnq1 cis* genes are abrogated in $Ezh2^{m-z-}$ and $Rnf2^{m-z-}$ extraembryonic tissues, despite the maintenance of the repressive compartment. Genomic contraction may be required for recruitment of *cis* genes into the repressive compartment, thereby contributing to full imprinted repression. The timing of development is indicated in hours (hrs).

and allelic exclusion (Roldan et al., 2005; Skok et al., 2007). Since Yy1, an evolutionarily conserved interactor of PRC2, is required for *Igh* locus contraction (Liu et al., 2007), and given the recently reported role for human EZH2 in genome-wide long-range chromosomal interactions (Tiwari et al., 2008), the PRC2 and PRC1 complexes are likely universal regulators of higher-order genomic organization during mammalian development.

EXPERIMENTAL PROCEDURES

Mice and Embryos

The generation of maternally and zygotically deficient ($Ezh2^{m-z-}$ and $Rnf2^{m-z-}$) embryos was performed as previously described (Puschendorf et al., 2008; van der Stoop et al., 2008). To discriminate between parental alleles, conditionally deficient males ($Ezh2^{F/F}$ or $Rnf2^{F/F}$ *Prrm1*−Cre/+) were made congenic for *Mus. spretus* at distal chromosome 7 by crossing with SD7P11 mice (Dean et al., 1998). All experiments were performed in accordance with the Swiss animal protection laws and institutional guidelines. Early mouse embryos were obtained from superovulated 6- to 10-week-old females mated with male studs according to standard procedures (Supplemental Data).

TS Cell Derivation and Maintenance

Trophectoderm stem cells (TS) were derived and maintained according to standard procedures described in Supplemental Experimental Procedures.

For assessing the stability of *Kcnq1ot1* ncRNA, TS cells were treated for 1 hr with 50 μg/ml 5,6-dichloro-1-β-D-ribofuranosylbenzimidazole (DRB) (Calbiochem, 287891). In recovery experiments, cells were washed after DRB treatment and cultured for 15 hr before RNA isolation.

FISH, Microscopy, and Image Analyses

FISH analyses were performed based on Chaumeil et al. (2006). Details on slides preparation, immuno-FISH and RNA-DNA FISH procedures, as well as antibodies and probes used are given in Supplemental Experimental Procedures. Image acquisition was performed using a laser scanning confocal microscope LSM510 META (Zeiss). Serial *z* series of 0.2 μm slices were recorded and deconvolution applied (Huygens from SVI) when necessary. TetraSpeck Fluorescent Microspheres (Invitrogen) were used to adjust alignments between channels. Confocal stacks were analyzed using Imaris (Bitplane) software. For measuring relative overlap of signals in immuno-RNA-FISH and RNA-DNA-FISH, a colocalization channel was created, analyzed in serial *z* optical series, and used for 3D reconstructions and numerical quantifications of overlap. For generating random spots in 3D confocal stacks, an algorithm was developed that generates random coordinates within the volume defined by the segmented DAPI nuclear staining (detailed in Supplemental Experimental Procedures). These in silico signals were used to verify association with different repressive marks.

Statistical Analysis

Measured distances between BAC RP23-16K9 and BAC RP23-473N24 FISH signals were normalized to the nuclear radius of individual nuclei. Significance of differences between sets of normalized distances were calculated using the one-sided exact Wilcoxon Mann-Whitney rank sum test as implemented in the package "coin" for R (www.r-project.org). The significance of differences in percent colocalization between RNA-FISH and DNA-FISH signals in WT and *Ezh2*$^{m-z-}$ cells was calculated similarly, using two-sided testing. For visualization, kernel density estimates for a Gaussian kernel were computed using R's density function and default bandwidth.

Allelic RT-PCR Analyses

Pools of E3.5 embryos or E6.5 embryonic and extraembryonic tissues were isolated from independent crosses after careful dissection of embryos at 6.5 days of development (E6.5). Care was taken to eliminate maternal tissue contaminations through successive washes in FHM media (Chemicon). Total RNA was extracted using the PicoPure RNA Isolation Kit (Arcturus Bioscience, Mountain View, CA), treated with DNaseI (Stratagene), and reversed transcribed by using oligo d(T)20 primers and SuperScript III Reverse Transcriptase (Invitrogen), according to the manufacturer's protocols. Semiquantitative analyses were performed as previously described (Lewis et al., 2006; Umlauf et al., 2004) (see Table S1). For quantitative analyses, primers that selectively amplify *Mus musculus* or *Mus Spretus* alleles were developed (Table S2), and real-time PCR was performed using the SYBR Green PCR Master Mix (Applied Biosystem) and ABI Prism 7000 Real-time PCR machine.

Allelic Chromatin Immunoprecipitation

Proliferating TS cell cultures were treated with cytoskeletal buffer (100 mM NaCl, 300 mM sucrose, 3 mM $MgCl_2$, 10 mM PIPES, 1 mM EGTA) including 0.5% Triton X-100 on ice for 5 min and then subsequently fixed in 1% PFA. Chromatin extracts were prepared as described previously (Stock et al., 2007). Antibodies used are described in Supplemental Experimental Procedures. Maternal (SD7) and paternal (C57Bl/6J) alleles were discriminated by PCR-SSCP analysis (Umlauf et al., 2004). Gels were stained with SYBR Gold (Invitrogen), and the fluorescence was detected on a Typhoon 9400 scanner (Amersham Biosciences) and quantified using ImageQuant software. The amount of precipitated material was calculated from the intensity of each band and normalized to the intensity of input. Primers and conditions used for allelic ChIP analyses are indicated in Table S3.

SUPPLEMENTAL DATA

Supplemental Data include three tables, ten figures, and Supplemental Experimental Procedures and can be found with this article online at http://www.developmentcell.com/cgi/content/full/15/5/668/DC1/.

ACKNOWLEDGMENTS

We thank Miguel Vidal, Haruhiko Koseki, Christian Seiser, and Thomas Jenuwein for providing antisera; Barbara Knowles and Robert Feil for making available *Zp3*-Cre transgenic mice and SD7P11 congenic mice, respectively. We thank Edith Heard and Julie Chaumeil for helpful technical advice. We acknowledge FMI colleagues Laurent Gelman, Jens Rietdorf, and Patrick Schwarb for excellent microscopy and imaging assistance; Aaron Ponti for generating the random-spot algorithm; Fred Zilbermann and Carolin Kolb for technical assistance and the FMI animal facility. We thank Ruth Williams, Philip Hublitz, and Dirk Schübeler for critical reading of the manuscript and all members of the Peters lab for fruitful discussions. R.T., S.Y., and A.H.F.M.P. conceived and designed the experiments. R.T. and S.Y. performed the experiments. R.T., S.Y., M.B.S., and A.H.F.M.P. analyzed the data. A.P.O. provided antibodies; M.v.L. and S.H.O provided *Rnf2* and *Ezh2* conditionally deficient mice, respectively. R.T. and A.H.F.M.P. wrote the manuscript. S.Y. is a recipient of a HFSP fellowship. Research in the Peters lab is supported by the Novartis Research Foundation and the NoE network "The Epigenome."

Received: April 1, 2008
Revised: July 1, 2008
Accepted: August 25, 2008
Published online: October 9, 2008

REFERENCES

Boyer, L.A., Plath, K., Zeitlinger, J., Brambrink, T., Medeiros, L.A., Lee, T.I., Levine, S.S., Wernig, M., Tajonar, A., Ray, M.K., et al. (2006). Polycomb complexes repress developmental regulators in murine embryonic stem cells. Nature *441*, 349–353.

Brown, K.E., Guest, S.S., Smale, S.T., Hahm, K., Merkenschlager, M., and Fisher, A.G. (1997). Association of transcriptionally silent genes with Ikaros complexes at centromeric heterochromatin. Cell *91*, 845–854.

Chaumeil, J., Le Baccon, P., Wutz, A., and Heard, E. (2006). A novel role for Xist RNA in the formation of a repressive nuclear compartment into which genes are recruited when silenced. Genes Dev. *20*, 2223–2237.

Dean, W., Bowden, L., Aitchison, A., Klose, J., Moore, T., Meneses, J.J., Reik, W., and Feil, R. (1998). Altered imprinted gene methylation and expression in completely ES cell-derived mouse fetuses: association with aberrant phenotypes. Development *125*, 2273–2282.

Fitzpatrick, G.V., Soloway, P.D., and Higgins, M.J. (2002). Regional loss of imprinting and growth deficiency in mice with a targeted deletion of KvDMR1. Nat. Genet. *32*, 426–431.

Green, K., Lewis, A., Dawson, C., Dean, W., Reinhart, B., Chaillet, J.R., and Reik, W. (2007). A developmental window of opportunity for imprinted gene silencing mediated by DNA methylation and the Kcnq1ot1 noncoding RNA. Mamm. Genome *18*, 32–42.

Katayama, S., Tomaru, Y., Kasukawa, T., Waki, K., Nakanishi, M., Nakamura, M., Nishida, H., Yap, C.C., Suzuki, M., Kawai, J., et al. (2005). Antisense transcription in the mammalian transcriptome. Science *309*, 1564–1566.

Kurukuti, S., Tiwari, V.K., Tavoosidana, G., Pugacheva, E., Murrell, A., Zhao, Z., Lobanenkov, V., Reik, W., and Ohlsson, R. (2006). CTCF binding at the H19 imprinting control region mediates maternally inherited higher-order chromatin conformation to restrict enhancer access to Igf2. Proc. Natl. Acad. Sci. USA *103*, 10684–10689.

Lanzuolo, C., Roure, V., Dekker, J., Bantignies, F., and Orlando, V. (2007). Polycomb response elements mediate the formation of chromosome higher-order structures in the bithorax complex. Nat. Cell Biol. *9*, 1167–1174.

Levine, S.S., King, I.F., and Kingston, R.E. (2004). Division of labor in polycomb group repression. Trends Biochem. Sci. *29*, 478–485.

Lewis, A., Mitsuya, K., Umlauf, D., Smith, P., Dean, W., Walter, J., Higgins, M., Feil, R., and Reik, W. (2004). Imprinting on distal chromosome 7 in the placenta involves repressive histone methylation independent of DNA methylation. Nat. Genet. *36*, 1291–1295.

Lewis, A., Green, K., Dawson, C., Redrup, L., Huynh, K.D., Lee, J.T., Hemberger, M., and Reik, W. (2006). Epigenetic dynamics of the Kcnq1 imprinted domain in the early embryo. Development *133*, 4203–4210.

Liu, H., Schmidt-Supprian, M., Shi, Y., Hobeika, E., Barteneva, N., Jumaa, H., Pelanda, R., Reth, M., Skok, J., Rajewsky, K., and Shi, Y. (2007). Yin Yang 1 is a critical regulator of B-cell development. Genes Dev. *21*, 1179–1189.

Mager, J., Montgomery, N.D., de Villena, F.P., and Magnuson, T. (2003). Genome imprinting regulated by the mouse Polycomb group protein Eed. Nat. Genet. *33*, 502–507.

Mancini-Dinardo, D., Steele, S.J., Levorse, J.M., Ingram, R.S., and Tilghman, S.M. (2006). Elongation of the Kcnq1ot1 transcript is required for genomic imprinting of neighboring genes. Genes Dev. *20*, 1268–1282.

Mohammad, F., Pandey, R.R., Nagano, T., Chakalova, L., Mondal, T., Fraser, P., and Kanduri, C. (2008). Kcnq1ot1/Lit1 noncoding RNA mediates transcriptional silencing by targeting to the perinucleolar region. Mol. Cell. Biol. *28*, 3713–3728.

Murakami, K., Oshimura, M., and Kugoh, H. (2007). Suggestive evidence for chromosomal localization of non-coding RNA from imprinted LIT1. J. Hum. Genet. *52*, 926–933.

Murrell, A., Heeson, S., and Reik, W. (2004). Interaction between differentially methylated regions partitions the imprinted genes Igf2 and H19 into parent-specific chromatin loops. Nat. Genet. *36*, 889–893.

Noordermeer, D., Branco, M.R., Splinter, E., Klous, P., van Ijcken, W., Swagemakers, S., Koutsourakis, M., van der Spek, P., Pombo, A., and de Laat, W. (2008). Transcription and chromatin organization of a housekeeping gene cluster containing an integrated beta-globin locus control region. PLoS Genet. *4*, e1000016.

Okamoto, I., Otte, A.P., Allis, C.D., Reinberg, D., and Heard, E. (2004). Epigenetic dynamics of imprinted X inactivation during early mouse development. Science *303*, 644–649.

Pauler, F.M., Koerner, M.V., and Barlow, D.P. (2007). Silencing by imprinted noncoding RNAs: is transcription the answer? Trends Genet. *23*, 284–292.

Peters, A.H., and Schubeler, D. (2005). Methylation of histones: playing memory with DNA. Curr. Opin. Cell Biol. *17*, 230–238.

Puschendorf, M., Terranova, R., Boutsma, E., Mao, X., Isono, K., Brykczynska, U., Kolb, C., Otte, A.P., Koseki, H., Orkin, S.H., et al. (2008). PRC1 and Suv39h specify parental asymmetry at constitutive heterochromatin in early mouse embryos. Nat. Genet. *40*, 411–420.

Rinn, J.L., Kertesz, M., Wang, J.K., Squazzo, S.L., Xu, X., Brugmann, S.A., Goodnough, L.H., Helms, J.A., Farnham, P.J., Segal, E., and Chang, H.Y. (2007). Functional demarcation of active and silent chromatin domains in human HOX loci by noncoding RNAs. Cell *129*, 1311–1323.

Roldan, E., Fuxa, M., Chong, W., Martinez, D., Novatchkova, M., Busslinger, M., and Skok, J.A. (2005). Locus 'decontraction' and centromeric recruitment contribute to allelic exclusion of the immunoglobulin heavy-chain gene. Nat. Immunol. *6*, 31–41.

Schoeftner, S., Sengupta, A.K., Kubicek, S., Mechtler, K., Spahn, L., Koseki, H., Jenuwein, T., and Wutz, A. (2006). Recruitment of PRC1 function at the initiation of X inactivation independent of PRC2 and silencing. EMBO J. *25*, 3110–3122.

Schulz, R., Menheniott, T.R., Woodfine, K., Wood, A.J., Choi, J.D., and Oakey, R.J. (2006). Chromosome-wide identification of novel imprinted genes using microarrays and uniparental disomies. Nucleic Acids Res. *34*, e88.

Shin, J.Y., Fitzpatrick, G.V., and Higgins, M.J. (2008). Two distinct mechanisms of silencing by the KvDMR1 imprinting control region. EMBO J. *27*, 168–178.

Skok, J.A., Gisler, R., Novatchkova, M., Farmer, D., de Laat, W., and Busslinger, M. (2007). Reversible contraction by looping of the Tcra and Tcrb loci in rearranging thymocytes. Nat. Immunol. *8*, 378–387.

Sleutels, F., Zwart, R., and Barlow, D.P. (2002). The non-coding Air RNA is required for silencing autosomal imprinted genes. Nature *415*, 810–813.

Stock, J.K., Giadrossi, S., Casanova, M., Brookes, E., Vidal, M., Koseki, H., Brockdorff, N., Fisher, A.G., and Pombo, A. (2007). Ring1-mediated ubiquitination of H2A restrains poised RNA polymerase II at bivalent genes in mouse ES cells. Nat. Cell Biol. *9*, 1428–1435.

Tiwari, V.K., Cope, L., McGarvey, K.M., Ohm, J.E., and Baylin, S.B. (2008). A novel 6C assay uncovers Polycomb-mediated higher order chromatin conformations. Genome Res. *18*, 1171–1179.

Umlauf, D., Goto, Y., Cao, R., Cerqueira, F., Wagschal, A., Zhang, Y., and Feil, R. (2004). Imprinting along the Kcnq1 domain on mouse chromosome 7 involves repressive histone methylation and recruitment of Polycomb group complexes. Nat. Genet. *36*, 1296–1300.

Umlauf, D., Fraser, P., and Nagano, T. (2008). The role of long non-coding RNAs in chromatin structure and gene regulation: variations on a theme. Biol. Chem. *389*, 323–331.

van der Stoop, P., Boutsma, E.A., Hulsman, D., Noback, S., Heimerikx, M., Kerkhoven, R.M., Voncken, J.W., Wessels, L.F., and van Lohuizen, M. (2008). Ubiquitin E3 ligase Ring1b/Rnf2 of polycomb repressive complex 1 contributes to stable maintenance of mouse embryonic stem cells. PLoS ONE *3*, e2235.

Wagschal, A., Sutherland, H.G., Woodfine, K., Henckel, A., Chebli, K., Schulz, R., Oakey, R.J., Bickmore, W.A., and Feil, R. (2008). G9a histone methyltransferase contributes to imprinting in the mouse placenta. Mol. Cell. Biol. *28*, 1104–1113.

Wiblin, A.E., Cui, W., Clark, A.J., and Bickmore, W.A. (2005). Distinctive nuclear organisation of centromeres and regions involved in pluripotency in human embryonic stem cells. J. Cell Sci. *118*, 3861–3868.